This is an open access article published under an ACS AuthorChoice License, which permits copying and redistribution of the article or any adaptations for non-commercial purposes.

analytical chemistry

Editors' Highlight

pubs.acs.org/ac

Specific Visualization and Identification of Phosphoproteome in Gels

Linna Wang,[†,§] Li Pan,[‡,§] and W. Andy Tao*[,†,‡,§]

[†]Department of Biochemistry, [‡]Department of Medicinal Chemistry & Molecular Pharmacology, and [§]Center for Cancer Research, Purdue University, West Lafayette, Indiana 47907, United States

Supporting Information

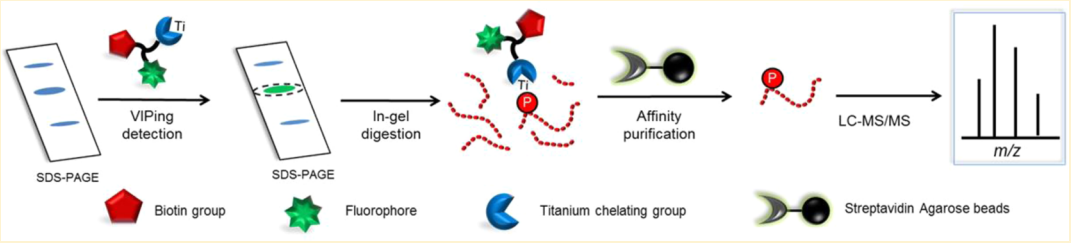

ABSTRACT: The applicability of gel-based proteomic strategies in phosphoproteomics has been largely limited by the lack of technologies for specific detection of phosphoproteins in gels. Here for the first time we report a strategy for simultaneous visualization and identification of phosphoproteome in gels (VIPing) through coupling specific detection of phosphoproteins with protein identification and phosphorylation site mapping by tandem mass spectrometry. The core of the strategy is a novel compound multifunctionalized with a titanium ion(IV) for outstanding selectivity toward phosphorylated residues, a fluorophore for visualization, and a biotin group for phosphopeptide enrichment. The sensitivity and specificity of the VIPing strategy was demonstrated using standard protein mixtures and complex cell extracts, and the method was applied to study the phosphorylation changes of an essential tyrosine kinase Syk and interacting proteins upon B-cell stimulation. The novel technique provides a powerful platform for gel-based phosphoproteomic studies.

Gel-based proteomic strategies, which often combine protein separation by one- or two-dimensional polyacrylamide gel electrophoresis (1D or 2D-PAGE) with protein identification by mass spectrometry (MS), pioneered the field of proteomics and used to be the workhorse in proteomic studies.[1−3] However, for the past decade, gel-free shotgun proteomics has become the major strategy for in-depth proteomic analyses. Thousands or even tens of thousands of proteins can be sequenced, frequently through multidimensional separation followed by mass spectrometric analysis. Large-scale studies on protein post-translational modifications (PTMs) such as phosphorylation are typically carried out by shotgun proteomics nowadays. Phosphoproteomics frequently requires extensive fractionation, phosphopeptide enrichment of each fraction, major instrument commitment, and integration of large data sets, even for a signaling event that may result in changes only in a few phosphoproteins, which becomes cost prohibitive for many researchers.

Here we revisit the gel-based strategy that may present cost-effective alternatives to gel-free large-scale phosphoproteomics. Gel-based analyses allow us to first visualize proteins in the gel and then only choose relevant proteins for in-gel digestion and mass spectrometric analysis. There have been several attempts to stain phosphoproteins in 1D and 2D gels,[4−6] such as Diamond ProQ[7,8] and PhosTag,[9] but highly abundant non-phosphorylated proteins can also be stained in previous studies.[3] Besides the lack of a more specific reagent to detect phosphoproteins in the gel as the major limitation of gel-based applications in phosphoproteomics, the finding of actual phosphopeptides is typically required to confidently identify a phosphoprotein. Because of the relatively low stoichiometric nature and ionization efficiency of phosphopeptides in mass spectrometric analysis, an efficient enrichment step is strongly recommended in phosphoproteomic studies. The most common enriching strategies are based on metal ion affinities to capture peptides containing negatively charged phosphate groups, such as immobilized metal affinity chromatography (IMAC), metal oxide affinity chromatography (MOAC),[10,11] and polymer-based metal ion affinity capture (PolyMAC).[12] Among the many metal ions employed, titanium ion (IV) has been demonstrated to be of superior specificity for phosphate groups.[13]

Here we devise a multifunctionalized molecule, termed visualization and identification of phosphoproteins in gels (VIPing), that combines gel-based phosphoprotein detection in high specificity with efficient phosphopeptide enrichment. Each VIPing molecule consists of a titanium ion for selective binding to phosphorylated residues, a fluorophore for visualization, and a biotin group to isolate phosphopeptides. The capability of the VIPing reagent was demonstrated with standard protein mixtures and complex samples by specifically staining phosphoproteins in gels and capturing phosphopeptides after

Received: May 5, 2014
Accepted: June 18, 2014
Published: June 18, 2014

 © 2014 American Chemical Society dx.doi.org/10.1021/ac501641u | *Anal. Chem.* 2014, 86, 6741−6747

in-gel digestion. The VIPing method was applied to study the phosphorylation changes of an essential tyrosine kinase Syk (spleen tyrosine kinase) and its interacting proteins upon B-cell stimulation.

EXPERIMENTAL SECTION

Experimental details in materials and the synthesis of VIPing reagent are included in the Supporting Information.

Phosphoprotein Detection and Phosphopeptide Enrichment by VIPing. Protein mixtures, such as the standard protein mixture (bovine serum albumin (BSA), ovalbumin, β-casein, β-lactoglobulin), *Escherichia coli* lysate, and proteins immunoprecipitated from DT-40 cell lysates, were separated on a precast SDS-PAGE (Invitrogen NuPAGE Bis-Tris gels) at 180 V/gel at room temperature. Fixation was accomplished by treating the gels with 50% MeOH/10% AcOH twice, for 30 min and overnight, respectively. The SDS-PAGE was then soaked in ddH_2O (three times, 10 min each) and incubated for 1 h with 1 μM of the VIPing reagent in 10 mL of 500 mM glycolic acid/1% TFA solution, pH 0.75. The gel was washed four times with 15 mL of 500 mM glycolic acid/1% TFA/20% CH_3CN solution for 30 min each wash and then twice with ultrapure water at room temperature for 5 min each wash. For detection, the gel was visualized using Typhoon FLA 9500 at an excitation source of 532 nm and emission filter of 580 nm. Sypro Ruby staining for total protein detection was performed on the same gel by following the product procedure. In-gel digestion with trypsin was conducted according to the method described by Mathris.[14] Tryptic peptides were extracted from the gel. The extraction was dried completely in SpeedVac. The peptide mixture was redissolved in 100 μL of 100 mM glycolic acid/1% TFA/50% CH_3CN. Another 1.4 pmol of VIPing was supplemented to the peptide mixture and incubated for 5 min. A volume of 200 μL of 300 mM HEPES (pH 7.7) was added to adjust to a final pH of 6.3. The solution was then transferred into a spin column with filter containing 10 μL of streptavidin beads (high capacity streptavidin agarose from Pierce). The spin column was gently agitated for an additional 30 min. The supernatant was removed from the spin column by centrifugation at 2000*g* for 30 s. The beads were then washed three times with 200 μL of 100 mM HOAc/80% CH_3CN for 5 min each. The peptides captured were eluted by incubation of the beads twice with 100 μL of 400 mM ammonium hydroxide solution for 5 min each. The eluates were collected and dried down completely under vacuum.

Phosphoprotein Dephosphorylation. For protein dephosphorylation, the protein mixture was incubated with calf intestine alkaline phosphatase (CIAP) in 1× CIAP buffer (50 mM Tris-Cl, 100 mM NaCl, 10 mM $MgCl_2$, 1 mM dithiothreitol) for 12 h at 37 °C. To stop the enzyme activity, the samples were boiled for 5 min in 1× SDS sample buffer.

Cell Culture. *E. coli* cells (strain: BL21) were grown in 250 mL of Luria–Bertani (LB) medium under vigorous shaking. At OD600 = 1.0, the cells were precipitated by centrifugation (10 min at 5000*g*) and resuspended in lysis solution (50 mM Tris-HCl, pH 7.5, 150 mM NaCl, 5 mM EDTA, 1% NP-40, 1× protease inhibitor cocktail) for 20 min on ice. Cells were lysed in lysis solution. Cells debris was cleared at 14 000*g* for 10 min. Supernatant containing soluble proteins was collected. The protein concentration of the cell lysate was determined using the Bicinchoninic acid (BCA) protein assay.

Syk Complex Preparation. DT-40 cells that express Syk-EGFP were cultured in RPMI 1640 medium containing 10% fetal calf serum, 1% chicken serum, 100 U/mL penicillin, and 100 μg/mL streptomycin. Cells (1 × 1E7 cells/mL) were stimulated with pervanadate treatment (freshly made 0.1 M H_2O_2 and 0.1 M Na_3VO_4 and incubated for 10–20 min before use). The stimulation reactions were stopped by washing with ice-cold PBS buffer. Cells were lysed in lysis buffer (50 mM Tris-HCl, pH 7.5, 150 mM NaCl, 1% NP-40, 1 mM sodium orthovanadate, 1× phosphatase inhibitor cocktail (Sigma), 1× protease inhibitor cocktail, 10 mM sodium fluoride). The protein concentration of the cell lysate was determined using the Bicinchoninic acid (BCA) protein assay. A volume of 20 μL (50% slurry) of GFP nanotrap agarose resin (Chromotek) was added to 10 mg of protein mixture and incubated overnight with end-to-end rotation at 4 °C. After incubation, the beads/protein complex was washed three times with lysis buffer and once with H_2O. The bound proteins were eluted by boiling in 2× SDS solution containing 40 mM DTT for 5 min at 95 °C. The resulting samples (including the set-aside lysates) were run on an SDS-PAGE gel.

LC–MS/MS Analysis. The dried peptides were resuspended in 10 μL of 0.5% formic acid and injected into an Eksigent 2D Ultra nanoflow HPLC system. The reverse phase C18 was performed using an in-house C18 capillary column packed with 5 μm C18 Magic beads resin (Michrom; 75 μm i.d. and 30 cm of bed length). The mobile phase buffer consisted of 0.1% formic acid in ultrapure water with the eluting buffer of 100% CH_3CN run over a shallow linear gradient over 20 min with a flow rate of 300 nL/min. The electrospray ionization emitter tip was generated on the prepacked column with a laser puller (model P-2000, Sutter Instrument Co.). The Eksigent Ultra HPLC system was coupled online with a high-resolution hybrid linear ion trap Orbitrap mass spectrometer (LTQ-Orbitrap Velos; Thermo Fisher). The mass spectrometer was operated in the data-dependent mode in which a full-scan MS (from m/z 300–2000 with the resolution of 30 000) was followed by 20 MS/MS scans of the most abundant ions. Ions with charge state of 1+ were excluded. The mass exclusion time was 90 s. The LTQ-Orbitrap raw files were searched directly against database *Gallus gallus* with Syk *Mus musculus* (P48025) sequence (17 620 entries, obtained from www.uniprot.org) or *Bos taurus* (23 850 entries, obtained from www.uniprot.org) using a combination of SEQUEST algorithm and MASCOT on Proteome Discoverer (version 1.4; Thermo Fisher). Peptide precursor mass tolerance was set at 10 ppm, and MS/MS tolerance was set at 0.8 Da. Search criteria included a static modification of cysteine residues of + 57.0214 Da and a variable modification of + 15.9949 Da to include potential oxidation of methionine, and a modification of + 79.996 Da on serine, threonine, or tyrosine for the identification of phosphorylation. Searches were performed with full tryptic digestion and allowed a maximum of two missed cleavages on the peptides analyzed from the sequence database. False discovery rates (FDR) were set below 1% for each analysis. Proteome Discoverer generates a reverse "decoy" database from the same protein database, and any peptides passing the initial filtering parameters that were derived from this decoy database are defined as false positive identification. Phosphorylation site localization from CID mass spectra was determined by PhosphoRS scores.[15] For phosphopeptides with ambiguous phosphorylation sites, only one phosphorylation site with the highest score was selected for further data interpretation.

dx.doi.org/10.1021/ac501641u | *Anal. Chem.* 2014, 86, 6741–6747

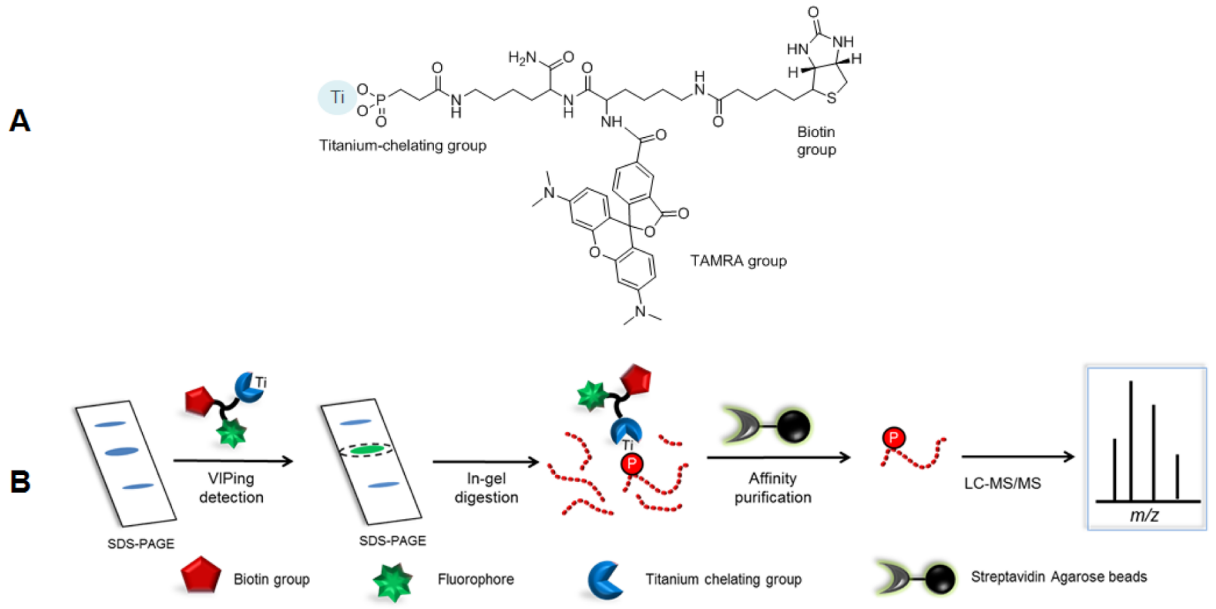

Figure 1. (A) Structure of VIPing reagent. VIPing consists of a titanium ion for selective binding to phosphate groups, a TAMRA for fluorescence-based detection and a biotin group for phosphopeptide purification via solid-phase capture. (B) Experimental workflow for VIPing strategy. After proteins are separated by SDS-PAGE, phosphorylated proteins are stained with VIPing reagent and then visualized with a fluorescence imager (Ex/Em = 532 nm/580 nm). The phosphorylated proteins of interest are excised in the gel and digested with trypsin. The phosphorylated tryptic peptides bound to the VIPing reagent are isolated via streptavidin beads followed by mass spectrometric analysis to identify the proteins and their phosphorylation sites.

RESULTS AND DISCUSSION

Design of VIPing Strategy. Our lab previously used a hyper-branched dendrimer-based bifunctional reagent, pIMAGO, containing biotin (bound with avidin-HRP for visualization) and phosphonate groups (for titanium ion chelation) to detect phosphoproteins on a membrane and in a 96-well plate.[16,17] We also devised a similar reagent, PolyMAC, containing aldehyde and phosphonate groups to allow for enriching phosphopeptides.[12] Both reagents, taking advantage of the stable titanium(IV) ion−phosphonate complex, demonstrated high specificity for the phosphate group. Unfortunately the dendrimer-based reagents are too big to be applied for in-gel analyses. We reason that trifunctional small molecules bind to phosphate groups on a phosphoprotein in the gel for in-gel detection and may be concurrently used for phosphopeptide enrichment after protein digestion prior to mass spectrometric analysis.

We devised a gel-compatible reagent, VIPing, which incorporates three independent functionalities: a titanium ion for highly selective binding to phosphate group, a fluorophore such as TAMRA for fluorescence-based detection, and a biotin group for phosphopeptide purification via solid-phase capture (Figure 1A). The VIPing reagent was prepared through solid-phase syntheses. Briefly, two lysine building blocks, Fmoc-Lys(Dde)−OH and Fmoc-Lys(Biotin)−OH were conjugated with rink beads consequently to form a compound with one biotin group and two orthogonal protected amine groups. After deprotection, the amine groups were reacted with TAMRA and *i*-Pro protected phosphonate groups separately. The product was cleaved from resin by acid cleaving, followed by removal of *i*-Pro groups with TMSBr. In the last step, the compound was functionalized with $TiOCl_2$ to generate the VIPing reagent.

The VIPing reagent is applied to the gel after SDS-PAGE separation to stain phosphoproteins and visualize with a fluorescence imager (Ex/Em = 532 nm/580 nm). The total protein detection, such as Sypro Ruby and Coomassie Blue, can be performed on the same gel for multiplexing as previously described.[18] The phosphorylated proteins of interest are excised in the gel and digested with trypsin. The tryptic phosphopeptides bound to the VIPing reagent are isolated via streptavidin beads followed by mass spectrometric analysis to identify the proteins and their phosphorylation sites (Figure 1B).

Selectivity and Sensitivity of VIPing-Based Detection. To initially investigate the ability of VIPing to selectively detect phosphorylated proteins in SDS-PAGE, we performed a gel staining of a five-protein mixture consisting of two standard phosphorylated (β-casein and ovalbumin) and three non-phosphorylated (BSA, catalase, and β-lactoglobulin) proteins. Five proteins of 500 ng each were mixed and separated by SDS-PAGE. Then the protein gel was incubated with the VIPing reagent and detected by a fluorescence imaging system. As shown in Figure 2A, only the two phosphoproteins (β-casein and ovalbumin) were stained in the protein gel, indicating good selectivity of VIPing toward phosphoproteins. Also as expected, the signal from β-casein appeared much stronger than that from ovalbumin, due to the relatively larger number of phosphorylated residues present in β-casein. The signals were no longer detectable after the proteins were treated with calf intestine alkaline phosphatase (CIAP). For comparison, the proteins were also detected by Sypro Ruby (a fluorescent dye for protein gel staining) subsequently on the same gel, as shown in Figure 2B. To further demonstrate the selectivity and sensitivity of VIPing-based phosphoprotein detection, the same five-protein mixture in different amounts, ranging from 7.85 ng to 250 ng were run in SDS-PAGE. The gel staining results (Figure 2C) indicated high specificity and sensitivity, allowing the detection of as low as 15 ng of β-casein. A comparison with Sypro Ruby staining (Figure 2D) indicates that VIPing has equivalent sensitivity to other fluorescence-based methods.

dx.doi.org/10.1021/ac501641u | *Anal. Chem.* 2014, 86, 6741−6747

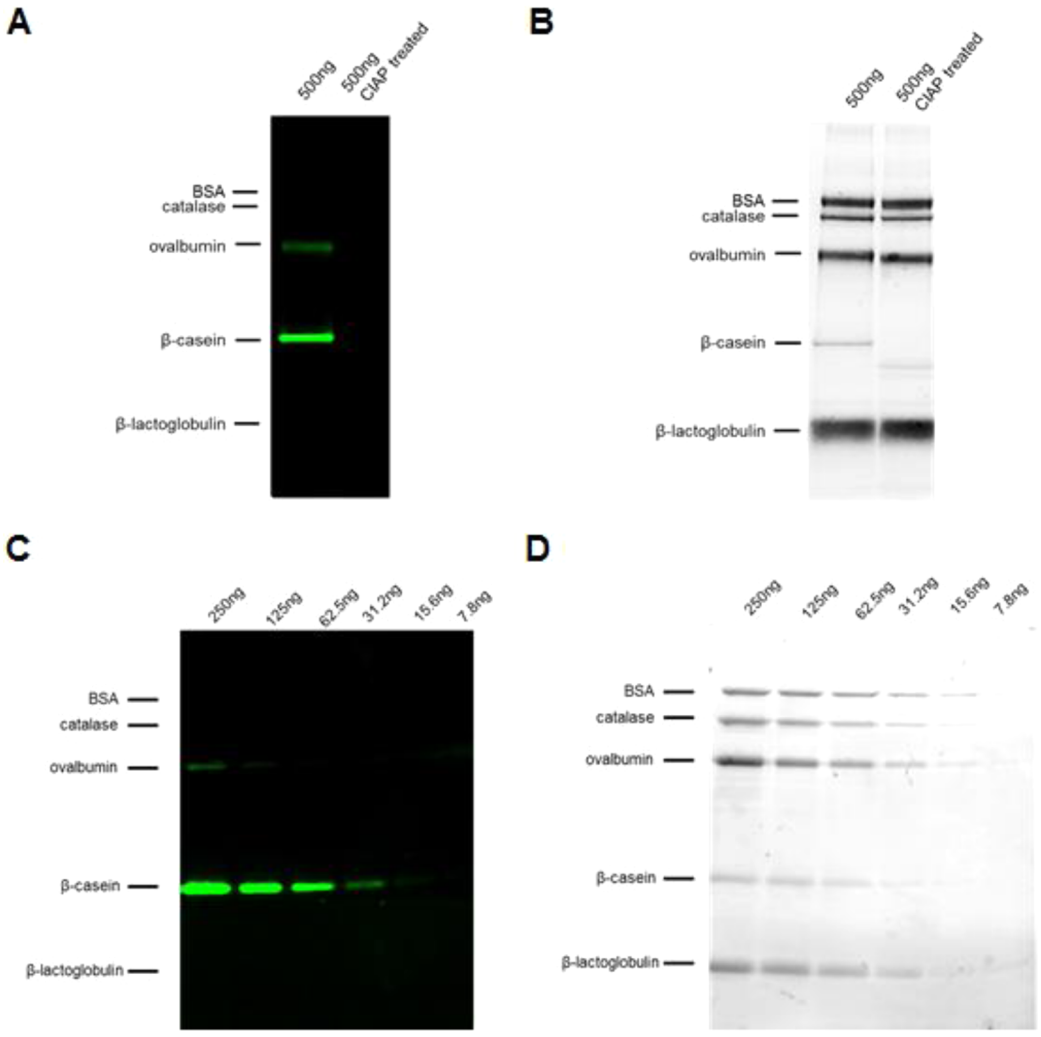

Figure 2. VIPing-based detection of phosphorylated proteins. Protein mixture includes three nonphosphorylated proteins (BSA, catalase, and β-lactoglobulin) and two phosphorylated proteins (ovalbumin and β-casein). (A) VIPing-based detection of 500 ng of the five-protein mixture with and without CIAP treatment. (B) Sypro Ruby-based protein detection of 500 ng of the five-protein mixture with and without CIAP treatment. (C) VIPing-based phosphorylation detection of different amounts of the five-protein mixture separated by SDS-PAGE. (D) Sypro Ruby-based protein detection of different amounts of the five-protein mixture separated by SDS-PAGE.

Next step, we explored the ability of VIPing to detect endogenous phosphorylated proteins in a whole cell extract of *E. coli* BL21 strain (Figure 3). The whole cell extract was also treated with CIAP. The CIAP-treated samples were equally divided and one was spiked with standard phosphoproteins, β-casein and ovalbumin. As shown in Figure 3A, VIPing was able to stain phosphoproteins in *E. coli* cell extract (Lane 1). The signals were due to protein phosphorylation since all signals disappeared when cell extract was treated with CIAP (Lane 2). Moreover, phosphoproteins β-casein and ovalbumin were clearly detected when spiking the five-protein mixture into CIAP-treated *E. coli* cell extract (Lane 3). Protein gel staining with Sypro Ruby indicates equal cell extract loading (Figure 3B).

Capture of Phosphopeptides from α-Casein with VIPing Strategy. Further, to investigate the ability of the VIPing reagent to enrich phosphopeptides, a similar standard containing phosphoprotein α-casein (mixture of isomers α-S1-casein and α-S2-casein) was applied to SDS-PAGE and visualized by VIPing. Following standard in-gel digestion, the phosphorylated peptides from α-casein bound to the VIPing reagent were isolated using solid-phase streptavidin beads and subjected to LC−MS/MS analysis. We also evaluated the capture efficiency of VIPing by streptavidin agarose beads. Using fluorescence detection, we were able to quantify the VIPing reagent present in the flow-through after solid phase capture. Only 2.22% of VIPing molecule was detected in the flow-through after streptavidin agarose capture, while more than 97% of VIPing molecule was successfully captured. In addition, less than 0.4% of VIPing reagent was found to be dissociated from streptavidin agarose during washing steps. More importantly, most phosphorylated peptides from α-S1-casein and α-S2-casein were identified by mass spectrometry (Table 1), demonstrating the capability of VIPing-based enrichment of phosphopeptides.

Detection of Endogenous Phosphorylation of Syk-Interacting Proteins. Finally, we applied the VIPing method to study the phosphorylation changes of an essential tyrosine kinase Syk and its interacting proteins that were coimmunoprecipitated from DT-40 chicken B cells upon pervanadate treatment. Syk is a nonreceptor cytoplasmic tyrosine kinase and plays a key role in mediating important cellular activities such as

dx.doi.org/10.1021/ac501641u | *Anal. Chem.* 2014, 86, 6741−6747

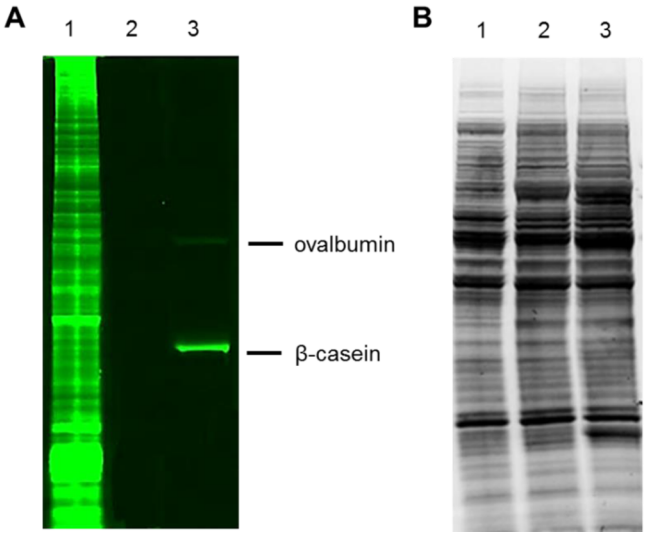

Figure 3. VIPing-based detection of endogenous phosphorylated proteins from *E. coli* whole cell extract. Lane 1, 25 μg of *E. coli* lysate protein; Lane 2, 25 μg of *E. coli* lysate protein with CIAP dephosphorylation treatment; Lane 3, 25 μg of *E. coli* lysate protein with CIAP dephosphorylation treatment and with 500 ng of the five-protein mixture spiked in. (A) VIPing-based detection of endogenous phosphorylated proteins from *E. coli*. (B) Sypro Ruby detection of *E. coli* lysate proteins with or without CIAP treatment.

cell adhesion, innate immune recognition, osteoclast maturation, platelet activation, and vascular development.[19,20] Moreover, Syk can function as a tumor promoter in hematopoietic malignancies and at the same time as a tumor suppressor in highly metastatic breast cancer and melanoma cells.[21] The stimulation of Syk leads to its autophosphorylation and increases its enzymatic activities, which in turn triggers a series of downstream phosphorylation events such as nuclear factor of activated T cells (NFAT) pathways and phosphoinositide-3-kinase (PI3K) mediated Tec family and Akt signaling pathways.

In this study, we employed DT-40 chicken B cells that express an exogenous Syk (*Mus musculus*) tagged with enhanced green fluorescent protein (Syk-EGFP) and treated the cells with pervanadate. Pervanadate is an irreversible protein-tyrosine phosphatase inhibitor and is known to enhance Syk phosphorylation in cells. To study phosphorylation changes of Syk and its interacting proteins upon pervanadate treatment, Syk-EGFP protein complex coimmunoprecipitated from DT-40 cells was subjected to SDS-PAGE analysis, followed by phosphoprotein gel staining using the VIPing reagent. After detection, phosphoproteins with significant phosphorylation changes were in-gel digested and analyzed with LC−MS/MS.

An anti-EGFP Western Blotting was carried out as the sample loading control (Figure 4A). As shown in Figure 4B, the

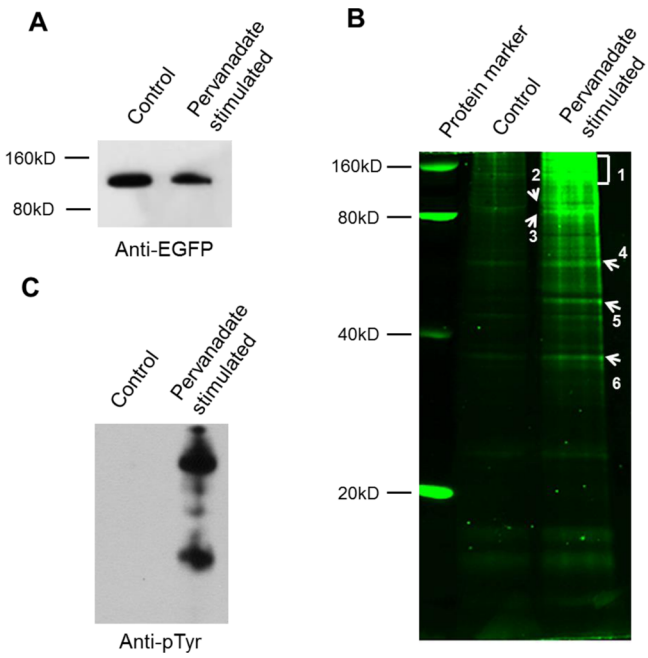

Figure 4. VIPing-based detection of phosphorylation in the EGFP−Syk protein complex coimmunoprecipitated from DT-40 cells with or without pervanadate stimulation. (A) Chemiluminescent HRP-anti-EGFP antibody detection, (B) VIPing-based phosphoprotein gel staining, and (C) chemiluminescent HRP-anti-pTyr antibody detection.

VIPing gel staining result indicates that the phosphorylation levels of both Syk and interacting proteins increased dramatically upon treatment. In parallel, the protein complex was also detected by an antiphosphotyrosine antibody, showing similarly increasing phosphorylation pattern for tyrosine phosphorylation (Figure 4C). All these data suggested the

Table 1. Phosphopeptides and Phosphorylation Sites of α-Casein Identified after VIPing-Based Phosphopeptide Enrichment

	phosphopeptide sequence	phosphorylated site	MH^+
α-S1-casein	DIGsEsTEDQAmEDIK	S4(Phospho); S6(Phospho)	1943.672 90
	DIGSEsTEDQAmEDIK	S6(Phospho)	1863.713 55
	VNELSKDIGsEsTEDQAmEDIK	S10(Phospho); S12(Phospho)	2614.041 29
	VPQLEIVPNsAEER	S10(Phospho)	1660.787 65
	KYKVPQLEIVPNsAEER	S13(Phospho)	2080.039 83
	EKVNELSKDIGsEsTEDQAmEDIK	S12(Phospho); S14(Phospho)	2871.167 33
	YKVPQLEIVPNsAEER	S12(Phospho)	1951.945 73
	YKVPQLEIVPNsAEERLHSmK	S12(Phospho)	2564.249 97
	VPQLEIVPNsAEERLHSmK	S10(Phospho)	2273.087 01
α-S2-casein	TVDMEsTEVFTK	S6(Phospho)	1466.606 61
	TVDmEsTEVFTK	S6(Phospho)	1482.603 56
	TVDMEsTEVFTKK	S6(Phospho)	1594.702 44
	TVDmEsTEVFTKK	S6(Phospho)	1610.697 07
	NmAINPsKENLcSTFcK	S7(Phospho)	2109.869 17

dx.doi.org/10.1021/ac501641u | *Anal. Chem.* 2014, 86, 6741−6747

Table 2. Phosphoproteins and Their Phosphorylation Sites Identified Using the VIPing Strategy

no.	protein name	phosphorylation site	ref[a]
1[b]	NFATc 3	LQSHKSyEGTSEVPESK	
		KTsEDQTATLSGK	12
	SMS-3	KGDVEGSQsQDEGEGSTESER	23
	NICE-4	RYPNSISsSPQKDLTQAK	24
	ACL	TAsFSESKPDDIAPAKK	24
	SDK1	SPPRPsPGGLHYsDEDICNK	
2[b]	SYK	ELNGTyAISGGR	25
		ADENYyK	26
	MCM3	QVEDDSEtEKEEEEEETQPEK	23
3[b]	HSP 90-β	IEDVGsDEEEEEGEK	27
4[b]	GAD1	EEFEMVFEGEPEHTNVCFWYIPPsLRGMPDCDER	
	NEDD8	FNLVVAtQLsEsTVLR	
5[b]	β-tubulin	IMNTFSVVPsPK	28
6[b]	UDG	SRsPEPGGDAEVTDDAAK	23

[a]The reference is for the corresponding phosphorylation sites on human or mouse homologue protein. [b]Band number marked in Figure 4B.

higher phosphorylation levels of Syk-EGFP and interacting proteins upon stimulation.

We selected six bands (marked in Figure 4B) that showed higher phosphorylation signals upon stimulation and carried out in-gel digestion, phosphopeptide enrichment by VIPing and analysis by LC−MS/MS. We identified a total of 14 unique phosphopeptides with 16 phosphorylation sites, representing 12 phosphorylated proteins, including Syk and several known Syk interacting proteins (Table 2). Among the 16 phosphorylation sites, two phosphorylation sites from Syk (*Mus musculus*) have been reported including Tyr 520, which is one of the known Syk autophosphorylation sites.[22] Nine phosphorylation sites from Syk-interacting proteins have also been reported on their corresponding *Homo sapiens* homologues; the other five phosphorylation sites are novel. All 12 identified proteins' *Homo sapiens* homologues are also known phosphoproteins. In addition, the molecular weights of the 12 identified phosphorylated proteins are consistent with their band positions in the gel. Therefore, the results indicated that the VIPing strategy is particularly appealing to detect novel phosphorylation events and characterize phosphorylation sites on endogenous proteins under different conditions without comprehensive phosphoproteomic analyses.

CONCLUSION

In summary, a novel technique that combines specific phosphoprotein detection in gels with phosphopeptide enrichment for confident identification of phosphoproteins was presented here. The VIPing strategy is highly specific for phosphoprotein visualization in SDS-PAGE, efficient for phosphopeptide enrichment, and compatible with mass spectrometric analysis. The technique can detect global changes in phosphorylation and is able to facilitate the identification of novel phosphorylated proteins and phosphorylation sites. The technology can be applied to detect phosphoproteome on the gel and then selectively identify phosphoproteins that are only relevant in a biological event. The technology allows multiplexed detection of phosphorylation and protein expression on the same gel when combined with total protein staining. The new strategy has the potential to be a major analytical tool for targeted phosphoproteomic studies.

ASSOCIATED CONTENT

Supporting Information

Additional information as noted in text. This material is available free of charge via the Internet at http://pubs.acs.org.

AUTHOR INFORMATION

Corresponding Author

*E-mail: taow@purdue.edu.

Notes

The authors declare no competing financial interest.

ACKNOWLEDGMENTS

This project has been funded in part by an NSF CAREER award (Grant CHE-0645020) and by National Institutes of Health Grant R01GM088317 (W.A.T.). We thank Dr. Robert. L. Geahlen and Wen-Horng Wang (Purdue) for generously providing *E. coli* BL21 strain and DT 40 cell lines.

REFERENCES

(1) Shevchenko, A.; Jensen, O. N.; Podtelejnikov, A. V.; Sagliocco, F.; Wilm, M.; Vorm, O.; Mortensen, P.; Boucherie, H.; Mann, M. *Proc. Natl. Acad. Sci. U.S.A.* **1996**, *93*, 14440−5.

(2) Rabilloud, T.; Lelong, C. *J. Proteomics* **2011**, *74*, 1829−41.

(3) Gorg, A.; Weiss, W.; Dunn, M. J. *Proteomics* **2004**, *4*, 3665−85.

(4) Jia, W.; Shaffer, J. F.; Harris, S. P.; Leary, J. A. *J. Proteome Res.* **2010**, *9*, 1843−53.

(5) Fristedt, R.; Granath, P.; Vener, A. V. *PLoS One* **2010**, *5*, e10963.

(6) Patwa, T. H.; Wang, Y.; Miller, F. R.; Goodison, S.; Pennathur, S.; Barder, T. J.; Lubman, D. M. *Proteomics Clin. Appl.* **2008**, *3*, 51−66.

(7) Steinberg, T. H.; Agnew, B. J.; Gee, K. R.; Leung, W. Y.; Goodman, T.; Schulenberg, B.; Hendrickson, J.; Beechem, J. M.; Haugland, R. P.; Patton, W. F. *Proteomics* **2003**, *3*, 1128−1144.

(8) Schulenberg, B.; Aggeler, R.; Beechem, J. M.; Capaldi, R. A.; Patton, W. F. *J. Biol. Chem.* **2003**, *278*, 27251−27255.

(9) Kinoshita, E.; Kinoshita-Kikuta, E.; Takiyama, K.; Koike, T. *Mol. Cell. Proteomics* **2006**, *5*, 749−57.

(10) Porath, J. *J. Chromatogr.* **1988**, *443*, 3−11.

(11) Neville, D. C.; Rozanas, C. R.; Price, E. M.; Gruis, D. B.; Verkman, A. S.; Townsend, R. R. *Protein Sci.* **1997**, *6*, 2436−45.

(12) Iliuk, A. B.; Martin, V. A.; Alicie, B. M.; Geahlen, R. L.; Tao, W. A. *Mol. Cell. Proteomics* **2010**, *9*, 2162−2172.

(13) Pinkse, M. W.; Uitto, P. M.; Hilhorst, M. J.; Ooms, B.; Heck, A. J. *Anal. Chem.* **2004**, *76*, 3935−3943.

(14) Shevchenko, A.; Tomas, H.; Havlis, J.; Olsen, J. V.; Mann, M. *Nat. Protoc.* **2006**, *1*, 2856−2860.

(15) Taus, T.; Kocher, T.; Pichler, P.; Paschke, C.; Schmidt, A.; Henrich, C.; Mechtler, K. *J. Proteome Res.* **2011**, *10*, 5354−5362.
(16) Iliuk, A.; Liu, X. S.; Xue, L.; Liu, X.; Tao, W. A. *Mol. Cell. Proteomics* **2012**, *11*, 629−639.
(17) Iliuk, A.; Martinez, J. S.; Hall, M. C.; Tao, W. A. *Anal. Chem.* **2011**, *83*, 2767−2774.
(18) Marondedze, C.; Lilley, K.; Thomas, L. *Methods Mol. Biol.* **2013**, *1016*, 139−154.
(19) Mocsai, A.; Ruland, J.; Tybulewicz, V. L. *Nat. Rev. Immunol* **2010**, *10*, 387−402.
(20) Geahlen, R. L. *Biochim. Biophys. Acta* **2009**, *1793*, 1115−27.
(21) Coopman, P. J.; Do, M. T.; Barth, M.; Bowden, E. T.; Hayes, A. J.; Basyuk, E.; Blancato, J. K.; Vezza, P. R.; McLeskey, S. W.; Mangeat, P. H.; Mueller, S. C. *Nature* **2000**, *406*, 742−747.
(22) Tsang, E.; Giannetti, A. M.; Shaw, D.; Dinh, M.; Tse, J. K.; Gandhi, S.; Ho, H.; Wang, S.; Papp, E.; Bradshaw, J. M. *J. Biol. Chem.* **2008**, *283*, 32650−32659.
(23) Grosstessner-Hain, K.; Hegemann, B.; Novatchkova, M.; Rameseder, J.; Joughin, B. A.; Hudecz, O.; Roitinger, E.; Pichler, P.; Kraut, N.; Yaffe, M. B.; Peters, J. M.; Mechtler, K. *Mol. Cell. Proteomics* **2011**, *10*, M111 008540.
(24) Hsu, P. P.; Kang, S. A.; Rameseder, J.; Zhang, Y.; Ottina, K. A.; Lim, D.; Peterson, T. R.; Choi, Y.; Gray, N. S.; Yaffe, M. B.; Marto, J. A.; Sabatini, D. M. *Science* **2011**, *332*, 1317−1322.
(25) Gu, T. L.; Deng, X.; Huang, F.; Tucker, M.; Crosby, K.; Rimkunas, V.; Wang, Y.; Deng, G.; Zhu, L.; Tan, Z.; Hu, Y.; Wu, C.; Nardone, J.; MacNeill, J.; Ren, J.; Reeves, C.; Innocenti, G.; Norris, B.; Yuan, J.; Yu, J.; Haack, H.; Shen, B.; Peng, C.; Li, H.; Zhou, X.; Liu, X.; Rush, J.; Comb, M. J. *PLoS One* **2011**, *6*, e15640.
(26) Ueki, Y.; Lin, C. Y.; Senoo, M.; Ebihara, T.; Agata, N.; Onji, M.; Saheki, Y.; Kawai, T.; Mukherjee, P. M.; Reichenberger, E.; Olsen, B. R. *Cell* **2007**, *128*, 71−83.
(27) Hengeveld, R. C.; Hertz, N. T.; Vromans, M. J.; Zhang, C.; Burlingame, A. L.; Shokat, K. M.; Lens, S. M. *Mol. Cell. Proteomics* **2012**, *11*, 47−59.
(28) Rigbolt, K. T.; Prokhorova, T. A.; Akimov, V.; Henningsen, J.; Johansen, P. T.; Kratchmarova, I.; Kassem, M.; Mann, M.; Olsen, J. V.; Blagoev, B. *Sci. Signal.* **2011**, *4*, rs3.